

Large bandwidth of NbN phonon-cooled hot-electron bolometer mixers on sapphire substrates.

S.Cherednichenko, P.Yagoubov, K.II'in, G.Gol'tsman, and E.Gershenson

Department of Physics, Moscow State Pedagogical University, Moscow 119435, Russia

ABSTRACT

The bandwidth of NbN phonon-cooled hot electron bolometer mixers has been systematically investigated with respect to the film thickness and film quality variation. The films, 2.5 to 10 nm thick, were fabricated on sapphire substrates using DC reactive magnetron sputtering. All devices consisted of several parallel strips, each 1 μ wide and 2 μ long, placed between Ti-Au contact pads. To measure the gain bandwidth we used two identical BWOs operating in the 120-140 GHz frequency range, one functioning as a local oscillator and the other as a signal source. The majority of the measurements were made at an ambient temperature of 4.5 K with optimal LO and DC bias. The maximum 3 dB bandwidth (about 4 GHz) was achieved for the devices made of films which were 2.5-3.5 nm thick, had a high critical temperature, and high critical current density. A theoretical analysis of bandwidth for these mixers based on the two-temperature model gives a good description of the experimental results if one assumes that the electron temperature is equal to the critical temperature.

INTRODUCTION

In recent years, significant advances have been made in the development of heterodyne receivers of a submillimeter waverange with a noise temperature approaching the quantum limit [1]. These receivers utilize Nb superconducting-insulator-superconducting (SIS) tunnel junction mixers. However, at frequencies higher than the energy gap for Nb (700 GHz) and especially higher than 1 THz the noise temperature grows drastically. Only Shottky diode mixers are used here, but they are much noisier and require a high local oscillator (LO) power.

Unlike direct detectors, conventional bolometers impose practically no restrictions as far as high frequencies are concerned, but these devices are slow and cannot be used as mixers. Although semiconducting hot-electron bolometers HEB (n-InSb) which appeared in the 60 s have a higher performance, they are still very far from being satisfactory for any major applications. The reason is that the intermediate frequency bandwidth (IF) is in this case limited to about 1 MHz. A substantial expansion of the bandwidth of the HEB mixers became possible when two-dimensional electron gas in GaAs/AlGaAs heterostructures were studied [2]. HEB mixers became much more promising after superconducting HEBs were developed [3]. In the devices of the latter type, when the electrons are phonon-cooled, the performance is in principle restricted by

the electron-phonon interaction time at a critical superconducting transition temperature $\tau_{\text{eph}}(T_c)$, which yields for an Nb mixer a bandwidth of about 500 MHz.

A further expansion of the bandwidth for this type of HEBs was made possible with the application of NbN, a superconducting material with a lesser time $\tau_{\text{eph}}(T_c)=15$ ps [4], which corresponds to about ~ 10 GHz mixer bandwidth. However, it is much more difficult to achieve a wide bandwidth for a HEB mixer than for a detector. To do so, ultrathin films with a high critical temperature T_c and critical current density $j_c(4.2\text{ K})$ must be available. The plane sizes have no impact whatever on the mixer bandwidth and can be randomly chosen to obtain the required values of the optimum LO power, dynamic range and impedance. As the NbN ultrathin film technology was developing, the HEB mixer bandwidth reached 1 GHz [5], then 2 GHz [6], and, finally, preliminary results were reported in [7] which included a bandwidth of 4 GHz accompanied by a low noise temperature at frequencies of 500-700 GHz and an optimal P_{LO} on the device $\sim 1\ \mu\text{W}$.

Another way of achieving a wide bandwidth of hot-electron bolometer mixers, the out-diffusion of hot electrons into normal metal leads, was proposed in [8] and implemented in [9]. This method does not require any changes in the superconducting material, a thinner film, or a high critical temperature (a Nb film 10 nm thick with $T_c=5\text{ K}$ proves to be quite satisfactory). However, very small in-plane sizes are a must: the length of the bridge should be as small as $0.08\ \mu$ for a 6 GHz bandwidth [10], which can be achieved using normal metal (100 nm thick Au) contacts and direct write e-beam lithography in a self-aligned process. Thus, for a diffusion-cooled HEB, the IF bandwidth appears to be connected with the LO power and the dynamic range of the mixer. For a 6 GHz bandwidth, $P_{\text{LO}}=10\ \text{nW}$ [10]. On the one hand, such a low value of LO power is an important issue at high submillimeter wave frequencies where LO power is difficult to generate. On the other hand, however, so small a dynamic range can be a problem since it can lead to an increase of a nonheterodyne response from thermal loading of the hot/cold loads [11].

In this paper we present the results of a systematic study of the bandwidth of phonon cooled NbN HEB mixer based on ultrathin films with high T_c and $j_c(4.2\text{ K})$ at a 140 GHz frequency.

EXPERIMENTAL

Ultrathin NbN films have been deposited on sapphire substrates by reactive dc magnetron sputtering in the Ar+N₂ gas mixture [12]. The maximum values of the critical film parameters (T_c and j_c) are reached at the discharge current value of 300 mA, the partial N₂ pressure of $1.7\cdot 10^{-4}$ mbar and the substrate temperature 850°C. The Ar pressure proved to have no substantial effect on the film deposition rate or film composition. For this reason, the pressure level was chosen in such a way as to maintain a stable discharge, namely $4.5\cdot 10^{-3}$ mbar. The deposition rate was 0.5 nm/s. It was

defined as a ratio of the film thickness, measured with a Talystep profilometer/profilograph, and its deposition time.

Fig. 1 gives the values of the critical temperature for the NbN film batch used in this work. The film thickness varies between 2.5 and 10 nm (Table 1). The thinnest films (2.5 nm thick) had T_c about 8.5 K and the transition width of about ~ 1.2 K. In the specified thickness range the sheet resistance of the films varied between 1000 and 70 Ohm/ \square , whereas the average resistivity was 150 $\mu\text{Ohm}\cdot\text{cm}$. The changes of these parameters during further contact metallization, ion milling and sputtering processes were insignificant.

Geometrically, NbN films in HEB mixers are several parallel strips 1 μ wide which are spaced 1 μ . For patterning, photolithography followed by ion milling was used. The strips were placed between Ti-Au contact pads 2-3 μ apart from each other. The number of NbN strips varied between 1 and 16 depending on the film thickness, to ensure that the normal state bolometer resistance stayed within the 200-300 Ohm range.

The experimental device was mounted on a waveguide flange, as shown on Fig. 2. The setup used for bandwidth measurements is presented in Fig. 3. Two backward wave oscillators (BWO) operating at 120-145 GHz were used as local oscillator and signal sources. The LO and signal radiation were coupled by a beam splitter and a beamguide into the cryostat. Two attenuators included in the quasioptical path line allowed to adjust the signal and LO power, and to maintain an optimum LO power during the retuning. The IF signal received from the mixer was amplified by a room temperature wideband amplifier (0.1-4 GHz) and was sent to the input of the spectrum analyzer.

The results of the investigations of the bandwidth of NbN HEB mixers are presented in Fig. 4-8. The data obtained under quasi-equilibrium conditions at $T \approx T_c$ allow the simplest interpretation and are at the same time quite informative of the physical processes responsible for the bandwidth. To obtain these data, low LO and dc powers were chosen: they were much lower than those optimal for mixing. In fact, a HEB mixer is functioning under these conditions as a direct detector for LO and signal beating oscillations. The results of these experiments demonstrate (Fig. 4) that the cut-off frequency is, respectively, 1.2 GHz, 2.8 GHz and 3.3 GHz for NbN mixer film thickness 10 nm, 5 nm and 4 nm. For thinner films, the cut-off frequency is approaching, or even exceeding, the upper limit of the measured frequency range (4 GHz).

The bandwidth of NbN HEB mixers in the optimal operating point at low temperature is often narrower than at $T \approx T_c$. The data for five mixers at $T=4.5$ K are given in Fig. 5. It can be seen that the bandwidth is growing as the films get thinner. However, practically no growth is observable for the thinnest films. It must be noted that the obtained bandwidth values for mixers made of thin films ($d=2.5-3.5$ nm) are only valid for high quality films. For films of a comparatively poor quality that had lower values of the critical temperature (T_c) and the critical current density (j_c) at $T=4.2$ K, the bandwidth is narrower than for quality films of the same thickness

(Fig. 6). At the same time, the data on the wide mixer bandwidth obtained at the 140 GHz frequency are fully confirmed by the measurements done at higher frequencies (660 GHz). In the latter experiments (Fig. 7) a quasi-optical mixer was used, which was made of a spiral antenna-coupled NbN HEB on a sapphire substrate. The results of bandwidth measurements of NbN HEB mixers on sapphire substrates are summarized in Fig. 8.

DISCUSSION

As was already mentioned, the results of bandwidth measurements taken at $T \approx T_c$ and P_{LO} and P_{dc} values much lower than those optimally required for the mixer are the simplest to interpret. Under these (quasi-equilibrium) conditions, the exact value of the electron temperature $\Theta = T = T_c$ is known, so one can be certain that the value of the self-heating parameter $C = I^2 \frac{\partial R / \partial \Theta}{c_e V} \tau_\Theta \ll 1$ (I is the bias current, c_e is the electron specific

heat, V is the volume of the mixer, $\tau_\Theta = \tau_{eph} + \frac{c_e}{c_{ph}} \tau_{es}$ is the electron temperature relaxation time, where c_{ph} is the phonon specific heat and τ_{es} is the phonon escape time). The latter fact allows to disregard a possible effect of the frequency dependence of mixer impedance in the intermediate frequency range close to $f \approx 1/2\pi\tau_\Theta$ as well as the feedback effect in the bias circuit [13]. For this reason, it is quite easy to calculate the frequency dependence of the amplitude of the variable constituent of the electron temperature $\Delta\Theta_{IF}(f)$ and hence the proportional IF voltage on the device within the two-temperature model [14]

$$U_{IF}(f) \sim \Delta\Theta_{IF}(f) = \frac{\Delta\Theta(0)(1 + j\omega\tau_0)}{(1 + j\omega\tau_1)(1 + j\omega\tau_2)}, \quad (1)$$

where $\tau_0^{-1} = \tau_{es}^{-1} + \tau_{eph}^{-1} c_e / c_{ph}$,

$$\tau_{1,2}^{-1} = \frac{\tau_{es}^{-1} + \tau_{eph}^{-1} (c_e / c_{ph} + 1)}{2} \left[1 \pm \sqrt{1 - 4 \frac{(\tau_{es}^{-1} + \tau_{eph}^{-1} (c_e / c_{ph} + 1))^2}{\tau_{es} \tau_{eph}}} \right],$$

$\tau_{es} = 13 \text{ ps} \cdot d(\text{nm})$ (see below), $\tau_{eph} = 5 \cdot 10^2 \cdot T^{-1.6} \text{ ps}$ [4], $c_e = 1.6 \cdot 10^{-4} \cdot T \text{ J/cm}^2 \cdot \text{K}$ [15], $c_{ph} = 9.8 \cdot 10^{-6} \cdot T^3 \text{ J/cm}^2 \cdot \text{K}$ [15].

For the thinnest NbN films used ($d = 2.5 \text{ nm}$), the escape time of the nonequilibrium phonons from the film into the substrate τ_{es} is much shorter than the time of their reabsorption by the electrons $\tau_{phe} = \tau_{eph} \frac{c_{ph}}{c_e}$. In this case the mixer bandwidth could be described by a single time constant τ_{eph} in a relatively simple hot electron model. However, for the thickest films used ($d = 10 \text{ nm}$), the τ_{es} and τ_{phe} times are close to each other and such a simplification would be too rough. As well be seen from the analysis

given below, the NbN films 3-3.5 nm thick which are now used to make practically operating HEB mixers also require that not only the electron but also the phonon heating should be considered, which means that the calculations must be carried out according to formulas (1).

Thorough experiments of bandwidth measurements and the comparison with the calculated data showed a very good correlation when the known τ_{eph} , c_e and c_{ph} values were used [15], but the τ_{es} value was somewhat different from that quoted in [15] for NbN films on sapphire. So, the curves 1-3 in Fig. 4 are produced according to (1) using $\tau_{\text{es}}=13 \text{ ps}\cdot\text{d}(\text{nm})$, while [15] quotes $\tau_{\text{es}}=8 \text{ ps}\cdot\text{d}(\text{nm})$. We believe that the difference is explained by more precise measuring of NbN film thickness in the present work.

We shall start the discussion of the results of the study of the NbN HEB in the optimum operating point at $T=4.5 \text{ K}$ with the mixers № 11 and 4 made of NbN films having 3.0-3.5 nm thick. The films of this quality and thickness seem to be a matter of the keenest practical interest. They have been used in HEB mixers studied in [7, 16]. It should be noted that the comparison of the bandwidth measurement results in the optimum operating point at frequencies of 140 and 660 GHz (Fig. 7) shows their full coincidence. Even though this result could be expected theoretically, it is nonetheless important because it demonstrates the practical applicability of the results obtained in the present work to terahertz range mixers. To compare the relative conversion gain vs intermediate frequency dependency with that theoretically calculated (Fig. 5) one needs to know the electron temperature value at the optimal point of the mixers. It can be defined by superimposing the IV curve under the optimal LO power on a set of IV curves derived for various ambient temperatures without a LO power. As can be seen in Fig. 9, a good correspondence may be obtained for the IV curve at $T=10 \text{ K}$. Taking into account that Joule power $P_{\text{dc}}=I_0\cdot V_0$, we can calculate an additional heating in the operating point $\Delta T_{\text{dc}}=0.5 \text{ K}$. The ultimate calculation of the electron temperature value in the operating point is $\Theta=10.5 \text{ K}$.

This Θ value can be now used to calculate the relative conversion gain vs intermediate frequency. The result gives a good description of the experimental data for this mixer. For other mixers, the above procedure of comparing IV curves was not applied, so the remaining curves are obtained by adjusting the calculations according to formulas (1) to the experimental data.

It is worthy of note that the high quality of the films and, specifically, the high critical temperature T_c and the high critical current density $j_c(4.2 \text{ K})$, along with the small thickness, is a necessary condition to ensure that the phonon-cooled HEB mixers have a wide bandwidth. This is illustrated by Fig. 6 where data are presented for three mixers with the same NbN film thickness ($d=3.0\text{-}3.5 \text{ nm}$). The № 4 mixer has high T_c and j_c values while the other two have lower values. It can be seen that the bandwidth of the latter two mixers is almost twice as narrow as that of the former mixer, this corresponds to the electron temperature $\Theta=5.5\text{-}5.7 \text{ K}$. This value is much lower than the

T_c for these mixers. This fact may be accounted for by a uniformity of the NbN films used to manufacture the mixers.

Such NbN films (with lower T_c and j_c) usually have a granular structure with weak intergranular links, and the superconducting transition shows a "tail" at low temperatures. The critical current density of such films is lower than that of the homogeneous films. When the current flow is higher than the critical current, these films develop a resistance, which is due to the transition to the normal state of those granular areas which are close to weak links because the superconductivity is substantially suppressed in such areas. When the current is growing, this resistance may be high enough, even though the value of the current itself is essentially lower than for HEB mixers made from high quality films. A substantial part of the LO power cannot be applied to HEB mixers produced from granular films, either. The reason is that with the growth of the electron temperature j_c drops even more and the resistance growth is observed with a still lower current value. The bandwidth of such a mixer is comparatively narrow and corresponds to the electron temperature Θ , which is much lower than T_c (see Fig. 6). As the films become more homogeneous, the "tail" in the temperature dependence curve of the resistance is reducing and, most importantly, the critical current density is growing. For the best NbN films used in this work to produce HEB mixers, $j_c(4.2\text{ K})$ reaches the value of $4 \cdot 10^6\text{ A/cm}^2$ at $d=3.5\text{ nm}$, while the resistance drops almost to zero and keeps very close to T_c . Such uniform films lack granular structure with weak links, so the value of the critical current is defined by vortex tear-off from pinning centers. The resistance generated in such conditions at a low T brings an overheating and the film is divided into thermal domains in which Θ is much greater than T and is close to T_c . This corresponds to an unstable IV-curves area (Fig. 9), so the current drops while remaining practically the same when the voltage continues to grow (see Fig. 9). The absorption of a sufficiently high LO power heats the electron subsystem substantially, the IV curves become smooth and the film resistance is accounted for by a uniform viscous vortex flow. In this IV-curve the critical current is much lower, hence the optimal bias current of the mixer is also lower. It is however true, within a certain limit, that the higher the critical current for the unpumped device, the larger the value of the optimal P_{LO} , the closer to T_c is the electron temperature under the optimum conditions of the mixer and the wider the operating IF bandwidth.

This can be illustrated by Fig. 8, which summarizes the measurement data and gives a dependency curve of 3 dB bandwidth calculation, which was produced using frequency dependencies (1). When calculating this curve, we assumed that the electron temperature Θ was equal to T_c , and experimentally determined the dependency of the latter value on film thickness (Fig. 1). It is only natural that the data on the bandwidth given in Fig. 4 very well agree with the curve. However, the mixer bandwidth measured in the optimal operating point at $T=4.5\text{ K}$ does not always correspond to the curve. For example, the mixers № 1, 4 and 11 we obtain bandwidth values which are close to those

calculated. These mixers were produced from ultrathin high quality films. Mixers № 2 and 3 show a slightly narrower bandwidth. It could be observed (see Table 1) that the T_c and j_c for these mixers can be only a trifle lower than for mixers № 4 and 11. As shown in the above discussion, however, the difference is great for mixers № 12 and 13.

Mixers № 5-10, which were made of films 4-10 nm thick, deserve a special consideration. The experimental data show (Fig. 5, 8) that as the thickness is growing the systematic deviation of the measured mixer bandwidth in the optimal operating point at $T=4.5$ K from that predicted is getting all the greater (see the curve in Fig. 8). For the calculated frequency dependencies in Fig. 5 this fact is interpreted as a lowering of the electron temperature in the optimal point with the film thickness growth.

However, this additional bandwidth narrowing may be accounted for by other reasons. A possible reason is a dependence of the HEB mixer impedance on the frequency, which has so far not been taken into account at all. The most significant changes of the impedance module and phase, however, are occurred just in the frequency range close to the upper frequency boundary of the 3 dB bandwidth. These changes can have an impact on the results of the frequency measurement. In the present work, we did not measure the impedance and so are unable to offer any experimentally based conclusions as to how great such an impact could be.

Another possible reason of the disagreement between the experimental and the calculated result is self-heating of the mixer due to a feedback in the dc circuit. This phenomena is reflected in particular in the formula for the HEB mixer bandwidth

$$\Delta B_m = \Delta B \left(1 + C \frac{R - R_L}{R + R_L} \right)$$

where ΔB - is the 3 dB bandwidth calculated from frequency dependencies (1). A characteristic feature of the effect is that depending on the R_L/R ratio the mixer bandwidth can be narrower or wider than ΔB . This should become essential when the self-heating parameter C is getting closer to 1. In the experiments, however, when the operating point was shifted along the optimal IV-curve, no change in mixer bandwidth was observed. This may be due to the fact that the values of C do not approach 1 at any point and that $\Delta B_m = \Delta B$.

ACKNOWLEDGMENTS

This work has been supported by Russian Program on Condensed Matter (Superconductivity Division) under Grant № 93169. The authors wish to thank B.M. Voronov for his assistance in the fabrication of the devices.

REFERENCES

- [1] J.Carlstrom and J.Zmuidzinis "Millimeter and Submillimeter Techniques", in "Review of Radio Science 1993-1995", ed. W.R.Stone, Oxford, The Oxford University Press, 1996.
- [2] J.X.Yang, F.Agahi, D.Dai, C.Musante, W.Grammer, K.M.Lau, and K.S.Yngvesson, IEEE Trans. Microwave Theory Tech. **MTT-41**, 581, (1993).
- [3] E.M.Gershenson, G.N.Gol'tsman, I.G.Gogidze, Yu.P.Gousev, A.I.Elant'ev, B.S.Karasik, and A.D.Semenov, Sov. J.Superconductivity **3**, 1582 (1990).

- [4] Yu.P.Gousev, G.N.Gol'tsman, A.D.Semenov, E.M.Gershenson, R.S.Nebosis, M.A.Heusinger, and K.F.Renk, "Broadband Ultrafast Superconducting NbN Detector for Electromagnetic Radiation", *J.Appl.Phys.*, **75**, 7, 3695 (1994).
- [5] G.N.Gol'tsman, B.S.Karasik, O.V.Okunev, A.L.Dzardanov, E.M.Gershenson, H.Ekstrom, S.Jacobsson, E.Kollberg. "NbN Hot Electron Superconducting Mixers for 100 GHz Operation." *IEEE Transactions on Applied Superconductivity*, **5**, 2, 3065 (1995).
- [6] O.Okunev, A.Dzardanov, G.Gol'tsman, and E.Gershenson. "Performances of Hot-electron Superconducting Mixer for Frequencies Less Than the Gap Energy: NbN Mixer for 100 GHz Operation." *Proc. of the 6th Int. Symp. on Space Terahertz Tech.*, Caltech, Pasadena, 247, (1995),
- [7] P.Yagoubov, G.Gol'tsman, B.Voronov, S.Svechnikov, S.Cherednichenko, E.Gershenson, V.Belitsky, H.Ekstrom, E.Kollberg, A.Semenov, Yu.Gousev, K.Renk, "Quasioptical phonon-cooled NbN hot-electron bolometer mixer at THz frequencies", *Proc. of the 7th Int. Symp. on Space Terahertz Tech.*, Charlottesville, VA, 303, (1996),
- [8] D.E.Prober, "Superconducting terahertz mixer using a transition-edge microbolometer", *Appl. Phys. Lett.* **62**, 17, 2119, (1993).
- [9] A.Scalare, W.R.McGrath, B.Bumble, H.G.LeDuc, P.J.Burke, A.A.Verheijen, R.J.Schoelkopf, and D.E.Prober, "Large bandwidth and low noise in a diffusion-cooled hot-electron bolometer mixer", *Appl. Phys. Lett.* **68**, 11, 1558, (1996).
- [10] P.J.Burke, R.J.Schoelkopf, D.E.Prober, A.Scalare, W.R.McGrath, B.Bumble, and H.G.LeDuc, "Length scaling of bandwidth and noise in hot-electron superconducting mixers", *Appl. Phys. Lett.* **68**, 23, 3344, (1996).
- [11] A.Scalare, W.R.McGrath, B.Bumble, H.G.LeDuc, "Receiver Measurements at 1267 GHz using a Diffusion-Cooled Superconducting Transition-Edge Bolometer", presented at ASC, Pittsburgh, 1996. To appear in *IEEE Transactions on Applied Superconductivity* 1997.
- [12] P.Yagoubov, G.Gol'tsman, B.Voronov, L.Seidman, V.Siomash, S.Cherednichenko, and E.Gershenson, "The bandwidth of HEB mixers employing ultrathin NbN films on sapphire substrate", *Proc. of the 7th Int. Symp. on Space Terahertz Tech.*, Charlottesville, VA, 290, (1996),
- [13] B.S.Karasik and A.I.Elant'ev, "Analysis of the Noise Performance of a Hot-Electron Superconducting Bolometer Mixer", *Appl. Phys. Lett.* **68**, 853, (1996).
- [14] N.Perrin and C.Vanneste, "Response of superconducting films to a periodic optical irradiation", *Phys. Rev.* **B28**, 5150, (1983).
- [15] A.D.Semenov, R.S.Nebosis, Yu.P.Gousev, M.A.Heusinger, and K.F.Renk", *Phys. Rev.* **B52**, 581, (1995).
- [16] H.Ekstrom, E.Kollberg, P.Yagoubov, G.Gol'tsman, E.Gershenson, S.Yngvesson, "Gain and noise bandwidth of NbN hot-electron bolometric mixers", submitted to *Appl. Phys. Lett.*, (1997).

Table 1. Critical temperature T_c , critical current density at $T=4.2$ K $j_c(4.2$ K), film thickness d and 3 dB bandwidth for NbN HEB mixers ΔB .

	T_c , K	$j_c(4.2$ K), A/cm ²	d , nm	ΔB , GHz
1	8.5	$9.3 \cdot 10^5$	2.5	4
2	9.2	$1.0 \cdot 10^6$	3.0	3
3	9.8	$1.8 \cdot 10^6$	3.5	3
4	10.2	$1.1 \cdot 10^6$	3.5	3.5
5	10.3	$2.1 \cdot 10^6$	4	2.7
6	10.4	$1.6 \cdot 10^6$	4	2.5
7	11.8	$4.1 \cdot 10^6$	5	1.9
8	11.8	$3.9 \cdot 10^6$	5	1.8
9	14.2	$6.5 \cdot 10^6$	10	0.9
10	14.2	$1.3 \cdot 10^6$	10	0.9
11	11	$3.9 \cdot 10^6$	3.5	3.5
12	8.5	$7.0 \cdot 10^5$	3.5	1.8
13	8.5	$5.0 \cdot 10^5$	3.5	1.9

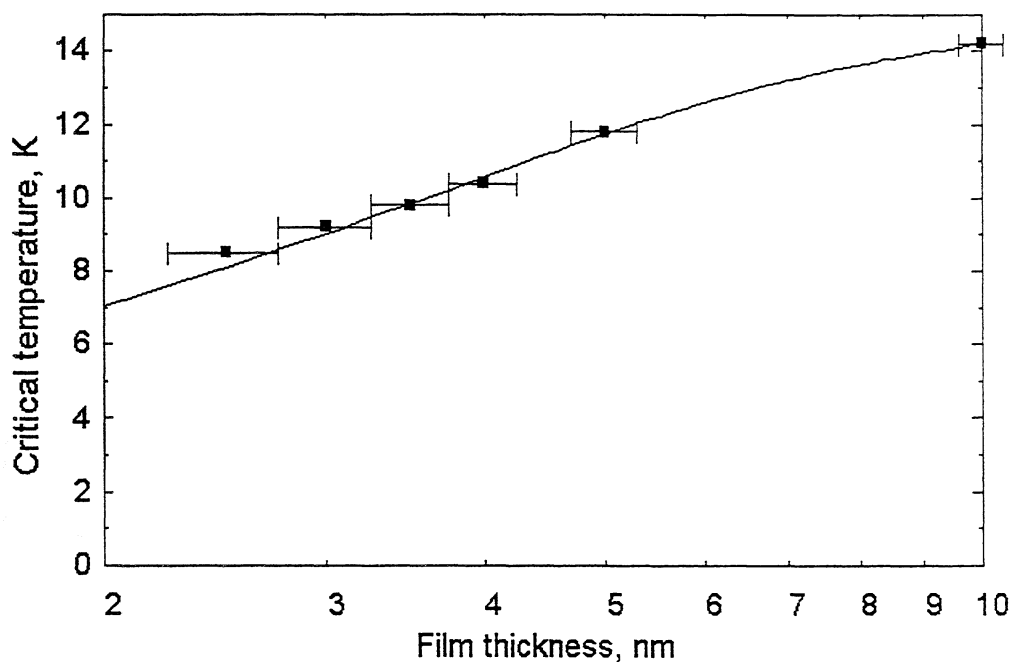


Fig. 1 Critical temperature vs film thickness (devices # 1, 2, 3, 6, 7, 9). The solid line is the typical $T_c(d)$ dependence for our films.

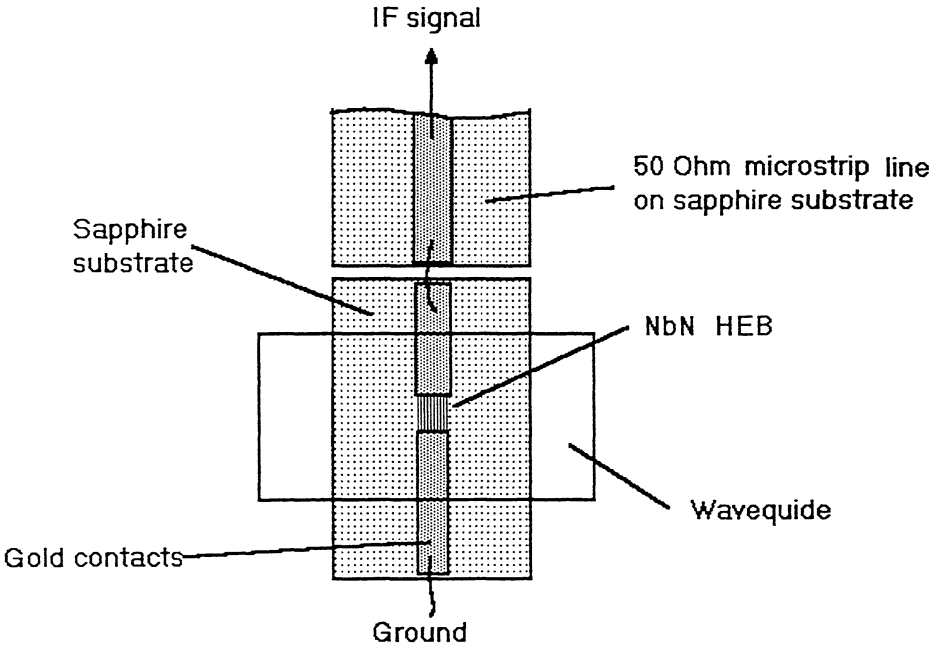


Fig. 2 View of the mixer chip on the waveguide flange.

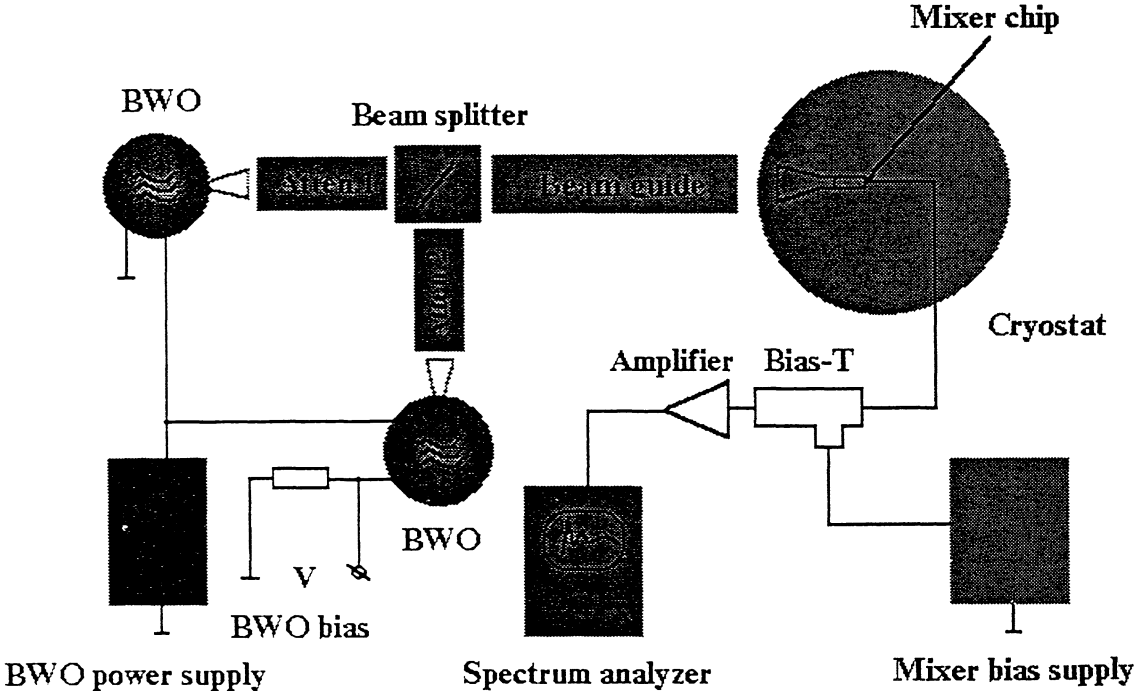


Fig. 3 Set-up for bandwidth measurements.

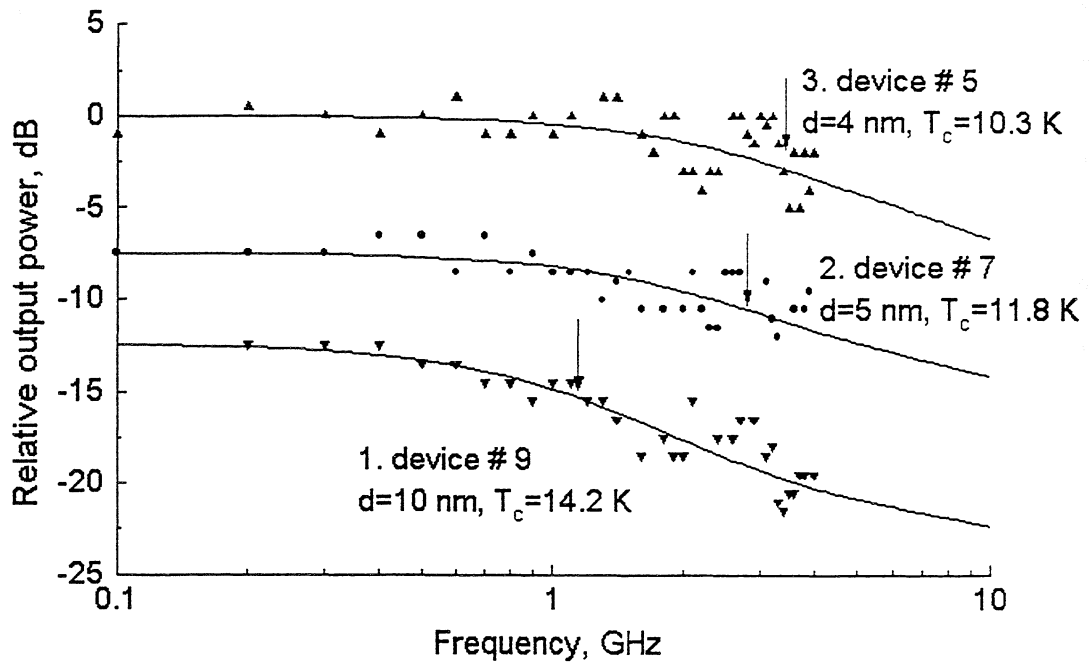


Fig. 4 Relative output power for devices #5, 7, 9 measured at $T = T_c$ (points) and calculated for $\Theta = T_c$ (solid line). The arrows show 3 dB cut-off frequencies.

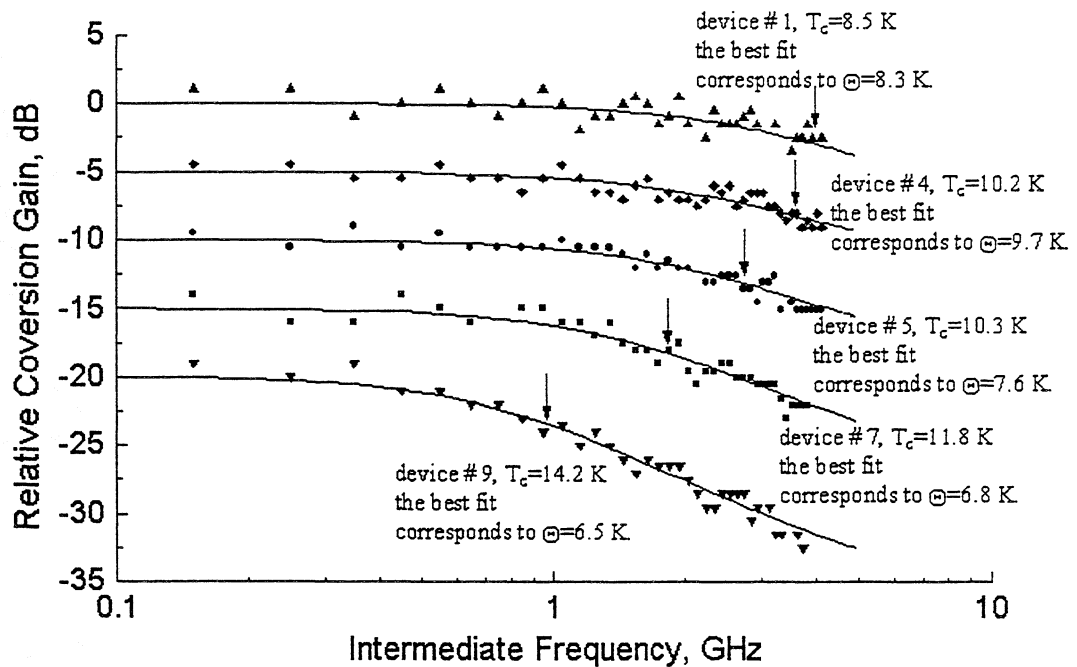


Fig. 5 Relative conversion gain for devices #1, 4, 5, 7, 9 measured at $T = 4.5$ K under optimal LO and dc bias; the arrows show 3 dB cut-off frequencies.

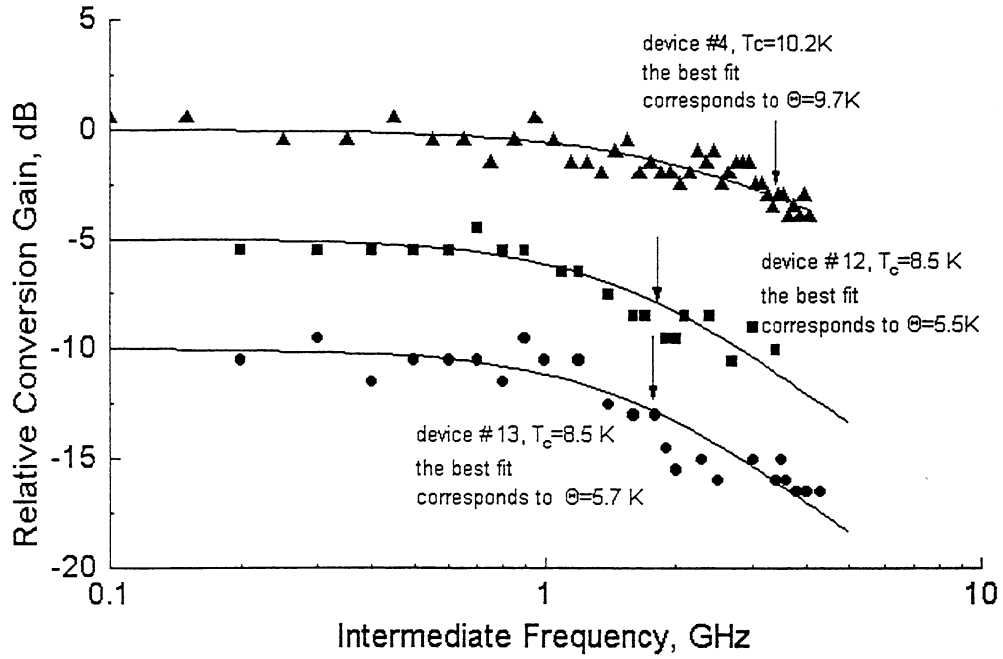


Fig. 6 Relative conversion gain for devices # 4, 12, 13 measured at $T=4.5$ K under optimal LO and dc bias; the arrows show 3 dB cut-off frequencies.

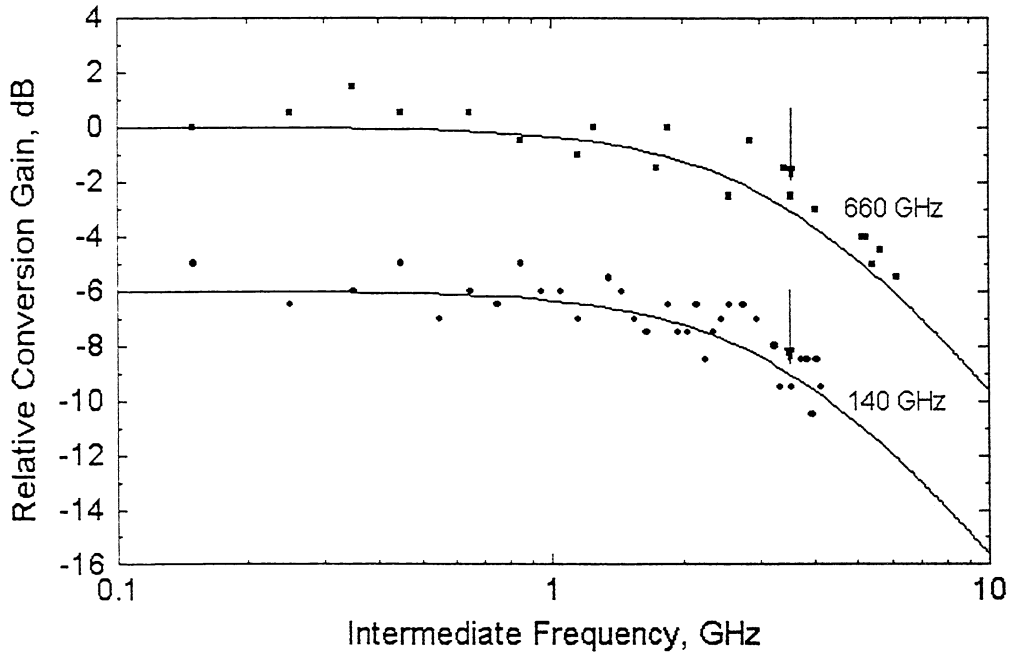


Fig. 7 Relative conversion gain for device # 11 measured at 140 and 660 GHz under optimal LO and dc bias.

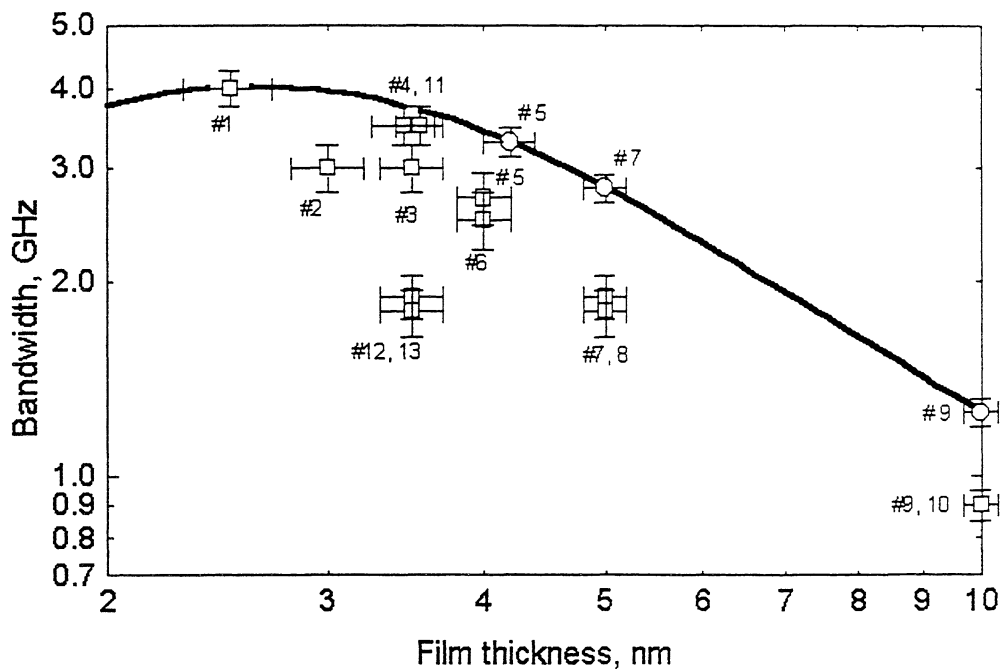


Fig. 8 3 dB bandwidth vs film thickness calculated taking into account $T_c(d)$ dependence typical for our films and experimental results for all devices at $T=4.5$ K, optimal P_{LO} and P_{dc} □; for three devices at $T=T_c$ small P_{LO} and P_{dc} ○.

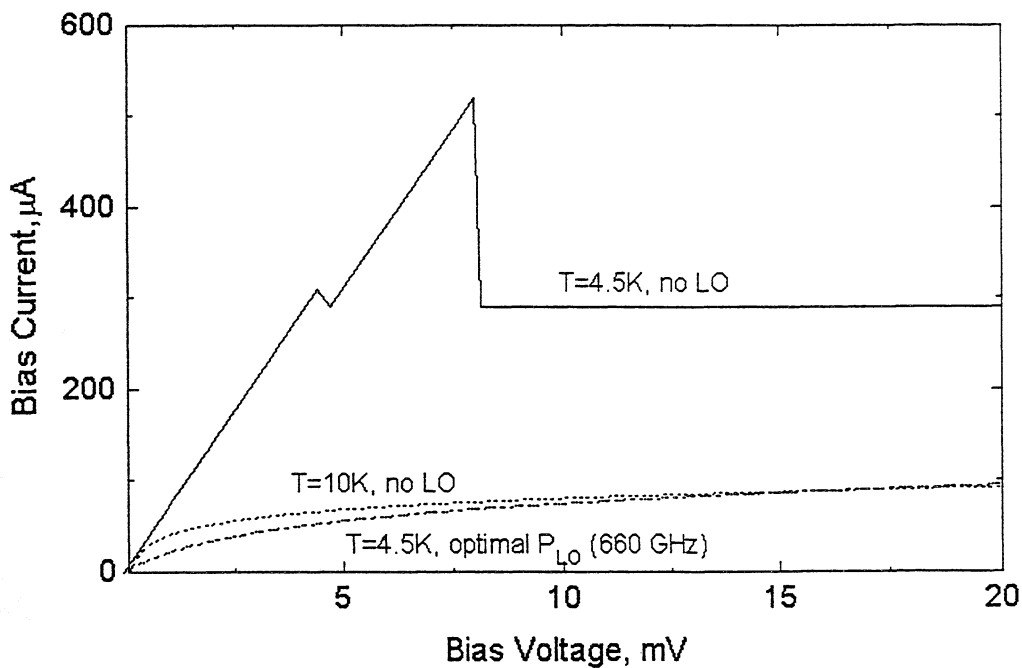


Fig. 9 IV-curves for device # 11.